

# Absorbing Boundary Conditions for Seismic Analysis in ABAQUS

Andreas H. Nielsen

Jacobs Babtie, 95 Bothwell St, Glasgow, UK

*Abstract: Absorbing boundary conditions are required to simulate seismic wave propagation in elastic media. In the first part of the paper, a number of relevant ABCs are reviewed with emphasis on practicality and ease of implementation. The second part of the paper describes the derivation of a new user element for seismic analysis in ABAQUS/Standard. The element is a combination of two ideas: one is the viscous boundary traction due to Lysmer and Kuhlemeyer, and the other is the free-field soil column as proposed by Zienkiewicz et al. The viscous boundary absorbs radiating waves, while the free-field soil column accounts for the seismic motions along the edges of the model. Element matrices are given in full.*

*Keywords: Absorbing Boundary Conditions, Dynamics, Free-field Boundary Conditions, Seismic Analysis, Soil-Structure Interaction, Wave Propagation, User Elements.*

## 1. Introduction

### 1.1 Background

Civil engineers use computer simulations to predict the response of structures subject to earthquake excitation. To keep the size of the computer model within practicable bounds, only a small portion of the ground influenced by the earthquake can be mapped onto a computational domain, while the rest has to be captured by an artificial boundary condition. The effect of an artificial boundary condition on the local response may be expected to diminish with distance according to Saint-Venant's principle. In static problems, fixed boundary conditions can be used without sacrificing much in terms of accuracy. In dynamic problems, fixed boundary conditions cause the reflection of outward propagating waves, effectively trapping energy inside the model. The simplest solution to this problem is to define a domain large enough so that waves reflected from the boundary do not have time to return to the region of interest. However, due to the relatively high wave speeds of most soils and rock, this is rarely a practical option. Therefore, it is desirable to have boundary conditions that allow the necessary energy radiation.

### 1.2 Outline of paper

On a number of recent commissions, ABAQUS has been used by Jacobs Babtie to model seismic problems in the time domain. In connection with this work, a desktop study was carried out to select and implement a suitable boundary condition for use in ABAQUS. This paper provides a

survey of the main findings. In Section 2 a few important results from the theory of wave propagation in elastic media are repeated. This section also serves to introduce the notation. A number of approximate solutions are reviewed in Section 3. The main features of the user element (UEL) subroutine of ABAQUS are summarised in Section 4. A new user element for seismic analysis in ABAQUS is derived in Section 5. This element effectively applies the *free-field boundary condition*, which was introduced in Section 3. Finally, a brief summary is given in Section 6.

## 2. Important results from the theory of wave propagation in elastic media

The wave equation for an isotropic elastic medium can be written as (Love, 1944)

$$c_p^2 \nabla(\nabla \cdot \mathbf{u}) - c_s^2 \nabla \times \nabla \times \mathbf{u} = \frac{\partial^2 \mathbf{u}}{\partial t^2}, \quad (1)$$

where  $c_p$  and  $c_s$  are constants defined below, and  $\mathbf{u}$  is the displacement vector,

$$\mathbf{u} = (u, v, w). \quad (2)$$

In an infinite medium, Equation (1) admits two and only two types of wave motion: primary (P) waves and secondary (S) waves. These waves propagate independently of each other and at different velocities. The P-wave is a dilatational wave involving no rotation, and the S-wave is a shear wave involving no dilatation. The P-wave velocity is given by

$$c_p = \sqrt{\frac{\lambda + 2\mu}{\rho}}, \quad (3)$$

and the S wave velocity is given by

$$c_s = \sqrt{\frac{\mu}{\rho}}, \quad (4)$$

where  $\lambda$  and  $\mu$  are the Lamé constants, and  $\rho$  is the density. Both P- and S- waves are classified as *body* waves.

When a boundary exists, the wave equation admits another class of waves called *evanescent* waves. These waves travel along the boundary between two media – in particular a free surface, in which case the name *surface* waves also applies. The motion decays exponentially in the direction normal to the boundary. Combinations of possible boundary conditions lead to a variety of these waves. In general, evanescent waves are *dispersive*, i.e. the wave velocity depends on frequency.

Boundaries not only act as waveguides for evanescent waves, they also couple the otherwise independently propagating dilatational and shear wave. It follows that the real difficulty in simulating seismic wave propagation not so much lies in the interior of the model, but at the artificial boundaries.

Two types of conditions must be satisfied on the surface of a wave front: kinematical and dynamical conditions (Love, 1944). In the two-dimensional case, kinematical conditions can be written as

$$\begin{aligned} \frac{1}{\cos \theta} \frac{\partial u}{\partial x} &= \frac{1}{\sin \theta} \frac{\partial u}{\partial y} = -\frac{1}{c} \frac{\partial u}{\partial t} \\ \frac{1}{\cos \theta} \frac{\partial v}{\partial x} &= \frac{1}{\sin \theta} \frac{\partial v}{\partial y} = -\frac{1}{c} \frac{\partial v}{\partial t} \end{aligned} \quad (5)$$

where  $\theta$  is the angle of incidence (see Figure 1), and  $c$  is the wave velocity. Dynamical conditions are given by

$$\begin{aligned} \rho c \frac{\partial u}{\partial t} &= -f_x \\ \rho c \frac{\partial v}{\partial t} &= -f_y \end{aligned} \quad (6)$$

where  $f_x$  and  $f_y$  are tractions applied to the surface  $dS$  of the interface, which is assumed to be coplanar with the wave front (see Figure 1).

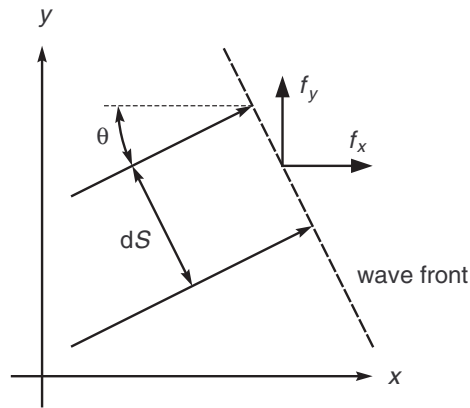


**Figure 1. Definition sketch.**

### **3. Review of existing solutions**

#### **3.1 Preliminary remarks**

Boundaries that do not reflect waves are called by various names: radiation boundaries, quiet boundaries, transmitting boundaries, absorbing boundaries, etc. Numerous solutions have been proposed in the last 35 years, and the literature on the subject is vast. Mulder (1997), Weber (1994), and Wolf (1988) all provide good introductions. This section reviews a small selection of the most promising methods that are available (in time domain). The aim is to select a suitable method for implementation in ABAQUS.

Three criteria guide us in the selection of a method. These criteria are:

1. Accuracy
2. Stability
3. Value for money

The first two criteria are mainly of academic concern and can be quantified with relative ease. The third criterion deserves a comment. The prediction of future earthquakes is associated with large uncertainty. As a consequence, the industry tends to favour conservative and robust methods of analysis and design, and shy overly complex and sophisticated methods that are difficult to validate and understand. It simply cannot be justified to employ methods having precision much greater than that of the input of the analysis. On the other hand, if both analysts and designers consistently err on the safe side, the resulting structure may be grossly overdesigned. Value for money, therefore, is broad criterion that guides to the middle ground between 'rule of thumb' and 'state of the art' analysis.

#### **3.2 Absorbing boundary conditions**

Most absorbing boundary conditions (ABCs) can be classified in two broad categories: global and local. In a global scheme, each boundary node is fully coupled to all other boundary nodes in both space and time. In a local scheme, the solution at any time step depends only on the current node and the current time step, and perhaps a few neighbouring points in time and space. Generally speaking, global boundaries are exact (although exact solutions are rarely attained in practice). Local boundaries are approximate, but appear much more attractive for numerical implementation than global boundaries.

The first local ABC was proposed by Lysmer and Kuhlemeyer (1969) who used viscous boundary tractions (dashpots) to absorb incident waves. For a vertical boundary defined by  $x = a$  the tractions can be written as

$$\begin{aligned} f_x &= -\rho c_p \frac{\partial u}{\partial t} \\ f_y &= -\rho c_s \frac{\partial v}{\partial t}. \end{aligned} \tag{7}$$

The boundary condition is completely effective at absorbing body waves approaching the boundary at normal incidence ( $\theta = 0$  in Figure 1). For oblique angles of incidence, or for evanescent waves, there is still energy absorption, but it is not perfect. Lysmer and Kuhlemeyer's viscous boundary is still one of the most popular methods today; it is widely used in industry, and it is the only absorbing boundary available in ABAQUS. The boundary condition is relatively easy to implement (see Section 5). An *implicit* viscous boundary is unconditionally stable (Cohen & Jennings, 1983). Moreover, given the large uncertainty associated with earthquake prediction, the accuracy of the method is acceptable for earthquake engineering purposes. However, it is still advisable to leave a relatively large margin between the boundary and the central region of the model.

Solutions published after Lysmer and Kuhlemeyer's classical paper (1969) are based on a variety of techniques. A majority of authors have aimed to devise a convenient mathematical approximation to the one-way wave equation, i.e. a governing equation that allows wave propagation in one direction only. One of the first solutions of this kind, and still one of the most accurate, was proposed by Lindman (1975) for the acoustic wave equation and extended by Randall (1988) to the elastic wave equation. The Lindman boundary absorbs both oscillating and evanescent waves. However, the procedure is developed for finite difference calculations and is not easily transferred into a finite element setting.

Engquist and Majda (1979) developed ABCs for elastic media based on a second-order Taylor expansion of the one-way wave equation around normal incidence ( $\theta = 0$ ). The second-order Taylor approximation leads to a formula with second-order derivatives. This situation is typical for the methods based on Taylor and Padé approximations: the resulting formulae contain derivatives up to the order of the approximation. The corresponding ABCs are said to have the same order as well.

Higdon (1990) devised a similar scheme from a different approach. Consider a wave travelling with velocity  $c$ . This wave approaches the boundary  $x = a$  at an angle of incidence  $\theta$ . According to Equation 5, an exact first-order boundary condition is given by

$$\left( \cos \theta \frac{\partial}{\partial t} + c \frac{\partial}{\partial x} \right) \mathbf{u} = 0. \tag{8}$$

It follows that the  $m$ th order boundary condition,

$$\prod_{j=1}^m \left( \cos \theta_j \frac{\partial}{\partial t} + c \frac{\partial}{\partial x} \right) \mathbf{u} = 0, \tag{9}$$

is a perfect absorber for waves approaching the boundary at  $m$  different angles of incidence.

Despite the appeal of increasing accuracy, the practical applications of high-order boundary conditions ( $m > 2$ ) are limited due to two reasons. Firstly, it is impossible, or at least very cumbersome, to define the high-order derivatives in a finite element formulation. Secondly, high-order boundary conditions suffer from stability problems (see Mulder, 1997, for a good introduction to this issue). Because of these limitations we are effectively left with the second-order boundary condition, i.e. Equation 9 with  $m = 2$ .

Users of FE software are faced with yet another problem. In ABAQUS, the UEL subroutine is probably the only extension with the required functionality for implementation of advanced boundary conditions. A user element must be defined in terms of force and stiffness. This requirement makes it difficult to implement Higdon's ABC, which is a *kinematical* boundary condition. To convert Equation 9 into a *dynamical* boundary condition, one could use Equation 6, but, in doing so, one would reintroduce the angle  $\theta$  into the equations, which is contrary to the original purpose of the approximation. The so-called *paraxial boundary* provides a way around this obstacle. In this method (Cohen & Jennings, 1983; Wolf, 1988), the governing one-way wave equation is recast in weak form; the weak form is integrated, and the structural matrices of a paraxial finite element are obtained. A boundary layer of paraxial elements around the main model works as an ABC. In theory, the paraxial boundary is more accurate than the viscous boundary. However, experience shows that the advantage of the paraxial boundary in actual implementations is slight (Cohen & Jennings, 1983).

In a recent paper Guddati (2006) derived a series of approximations to the one-way wave equation with increasing accuracy. The procedure is applicable to various types of material including anisotropic and porous elastic media, and it provides effective energy absorption over an arbitrarily wide range of incident angles. The basic idea (Guddati, 2000) is to eliminate the high-order spatial and temporal derivatives by use of auxiliary variables. These variables are interpreted as extra degrees of freedom and enter the global system of equations alongside the conventional degrees of freedom. The application of the boundary condition can be viewed as adding layers of elements around the artificial boundaries of the main model where energy radiation is required. One layer of elements provide perfect absorption of incident waves with wavenumber  $k$  when the 'width'  $L$  of the layer is defined as

$$L = \frac{2i}{k} \quad (10)$$

where  $i = \sqrt{-1}$ . When  $L$  is imaginary ( $k$  real), the layer captures mainly oscillating waves. When  $L$  is complex, the layer accommodates both evanescent and oscillating waves. By adding more layers with different  $L$  values, the method becomes increasingly accurate for all types of waves. The use of complex numbers to define the properties of an element results in complex system matrices. How this boundary condition can be incorporated into a direct integration algorithm based on real numbers, is not clear at the present stage. The stability properties of Guddati's ABC have not yet been demonstrated. Nevertheless, the scheme is one of the most promising local ABCs to emerge for finite element computations in the time domain.

### 3.3 Free-field boundary conditions

The boundary conditions reviewed so far were all designed to absorb outgoing waves. They can be used without further modification when the source of excitation is within the model (e.g. vibrating machinery). When the excitation originates from outside the model, for instance as an incoming seismic wave, the ABCs need to be extended. In earthquake engineering the incoming wave field is usually specified as a suite of independent orthogonal acceleration time histories. These histories are converted into time-varying tractions (via Equation 6) and applied to the base of the model where they become vertically propagating P- and S-waves.

Along the sides of the model, the motion is not known beforehand. In a method described by Zienkiewicz *et al.* (1989) and Wolf (1988), so-called free-field soil columns are defined on either side of the main model as illustrated in Figure 2. The columns are solved in parallel with the main model. The free-field motions are converted into boundary tractions, which are applied to the main model. The technique implies that information only travels from the free field to the main mesh, not vice versa. In this way, the response of the free field is not influenced by soil-structure interaction within the main model – a bold assumption, but probably justified if the columns are placed at some distance from the central region of the model.

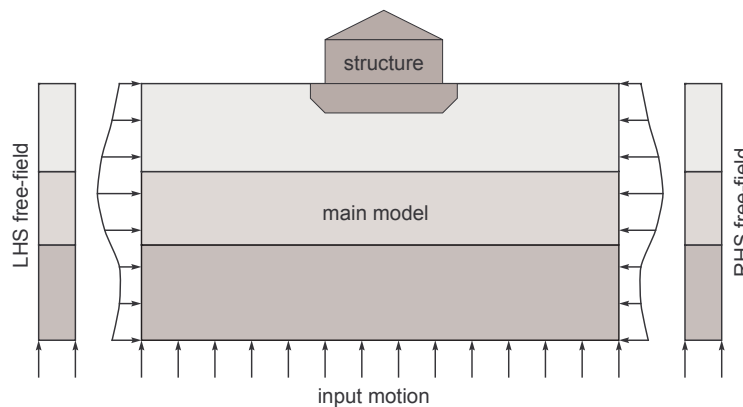


**Figure 2. Free-field boundary conditions.**

Together with a suitable ABC, the free-field columns provide a *free-field boundary condition*. Although conceptually simple, this scheme is not easy to implement because it involves two, or potentially three, parallel computations: one for the main model, and one for each soil column. However, the free-field boundary element presented in Section 5 avoids this difficulty.

## 4. User elements in ABAQUS

In ABAQUS/Standard, the most flexible feature for implementation of advanced boundary conditions is the user element (UEL) subroutine. Unfortunately, ABAQUS/Explicit does not have

a similar user subroutine at present. Users are therefore restricted to implicit dynamic analysis. In this section, the important features of the UEL subroutine are briefly summarised.

We now use  $\mathbf{U}$  to denote the displacement vector, which is discrete in time and space, as opposed to  $\mathbf{u}$ , which is continuous in time and space. The UEL subroutine must return element contributions to the residual  $\mathbf{F}$  and the Jacobian  $\mathbf{J}$ . ABAQUS uses the Hilber-Hughes-Taylor method for implicit integration of dynamic systems. In this method the residual at time  $t+\Delta t$  is defined as:

$$\mathbf{F}_{t+\Delta t} = -\mathbf{M}\ddot{\mathbf{U}}_{t+\Delta t} + (1+\alpha)\mathbf{G}_{t+\Delta t} - \alpha\mathbf{G}_t, \quad (11)$$

where  $\ddot{\mathbf{U}}_{t+\Delta t}$  is the acceleration vector at time  $t + \Delta t$ , and  $\alpha$  is a parameter that controls characteristics of the algorithm such as accuracy and numerical damping (typically  $\alpha = -0.05$ ). In the following we omit subscript  $t$  and  $t + \Delta t$ . The vector  $\mathbf{G}$  is referred to as the static residual. It is defined as

$$\mathbf{G} = \mathbf{P} - \mathbf{R}, \quad (12)$$

where  $\mathbf{P}$  are external nodal loads applied to the element, and  $\mathbf{R}$  are internal nodal forces that equilibrate elastic and viscous stresses within the element.

The Jacobian is defined as

$$\mathbf{J} = -\frac{d\mathbf{F}}{d\mathbf{U}}. \quad (13)$$

In other words, once the residual has been defined, the Jacobian follows by differentiation. For linear-elastic elements with structural matrices  $\mathbf{M}$ ,  $\mathbf{C}$ , and  $\mathbf{K}$  defined in the usual sense, the Jacobian may be written as:

$$\mathbf{J} = \frac{1}{\beta\Delta t^2}\mathbf{M} + (1+\alpha)\left(\frac{\gamma}{\beta\Delta t}\mathbf{C} + \mathbf{K}\right), \quad (14)$$

where the Newmark parameters  $\beta$  and  $\gamma$  are calculated from

$$\beta = \frac{1}{4}(1-\alpha)^2 \text{ and } \gamma = \frac{1}{2} - \alpha. \quad (15)$$

## 5. The free-field boundary element

### 5.1 Outline of method

The derivation of a new free-field boundary element is presented in this section. We have chosen to use Lysmer & Kuhlemeyer's viscous boundary tractions combined with a vertical free-field soil column. Based on the review in Section 3, this method seems to offer best value for money.

The total boundary traction is composed of two terms: one due to the viscous dashpots that absorb radiating energy, and one due to the free-field motion which is assumed to be undisturbed by the presence of irregularities within the main model. The normal and shear tractions,  $f_n$  and  $f_s$  respectively, are therefore written as

$$\begin{aligned} f_n &= \rho c_p \left( \frac{\partial u'}{\partial t} - \frac{\partial u}{\partial t} \right) + \ell_x \sigma'_x \\ f_s &= \rho c_s \left( \frac{\partial v'}{\partial t} - \frac{\partial v}{\partial t} \right) + \ell_x \tau'_{xy} \end{aligned} \quad (16)$$

where prime denotes quantities evaluated in the free-field,  $\ell_x = 1$  if an outward normal points in the positive  $x$  direction, and  $\ell_x = -1$  if an outward normal points in the negative  $x$  direction. The first term in Equation 16 is the traction due to dashpots as proposed by Lysmer and Kuhlemeyer (*cf.* Equation 7). The second term is the stress due to free-field wave propagation, plus any static reactions.

The remaining part of the section is divided into two subsections. First, in Section 5.2, the structural matrices for a two-node standalone soil column element are derived. Second, in Section 5.3, the matrices for a four-node free-field boundary element are derived based on the results in the previous subsection. The resulting formulae are valid for a vertical boundary. Similar expressions may be written for a horizontal boundary by interchanging  $x$  and  $y$ , and the associated degrees of freedom. The derivation assumes familiarity with basic finite element theory; readers are referred to the excellent textbook by Cook *et al.* (2002).

### 5.2 The soil column element

A soil column is used to analyse the response of horizontally layered soil/rock systems subject to vertically propagating S- and P-waves. A soil column admits solutions of the wave equation in the vertical ( $y$ ) direction only. Because of this restriction, a soil column element is particularly easy to formulate.

The element has height  $h$ , width  $b$ , and thickness  $t$ . The dimensions  $h$  and  $b$  are defined in Figure 3; the thickness  $t$  is the dimension normal to the plane of the paper. For convenience,  $b$  and  $t$  could be assigned unit length and omitted from all equations; however, they are included in the following derivation to enable unit checking. The element has two nodes numbered 1 and 4. Node  $n$  is associated with two degrees of freedom: displacements  $U_n$  and  $V_n$  (subscript  $t$  for time

step is omitted, but should be inferred). If the density of the material is  $\rho$ , the element mass is  $m = \rho h b d$ . A lumped mass matrix of the soil column is given by

$$\mathbf{M}' = \frac{m}{2} \mathbf{I}, \quad (17)$$

where  $\mathbf{I}$  is a 4x4 identity matrix.

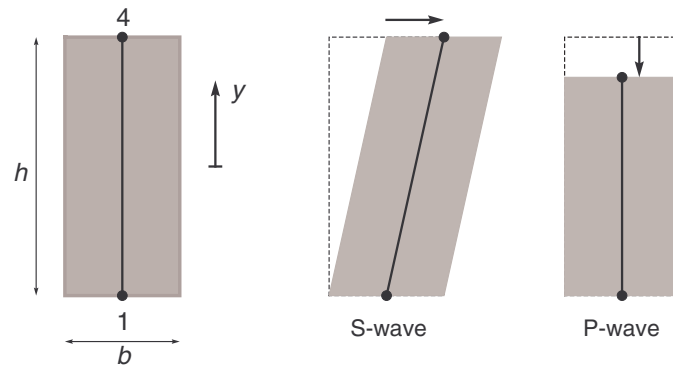


**Figure 3. A soil column element for flat sites with horizontal soil layers. Also shown are element deformations due to S- and P-waves respectively.**

Displacements are interpolated linearly in the element coordinate system  $y$  by shape functions  $N_1$  and  $N_4$  such that

$$\begin{aligned} u(y) &= N_1 U_1 + N_4 U_4 \\ v(y) &= N_1 V_1 + N_4 V_4 \end{aligned} \quad (18)$$

where

$$N_1 = \frac{(h-2y)}{2h}, \quad N_4 = \frac{(h+2y)}{2h}. \quad (19)$$

Strains are given by

$$\varepsilon_x = 0, \quad \varepsilon_y = \frac{dv}{dy}, \quad \gamma_{xy} = \frac{du}{dy}, \quad (20)$$

or, in the customary FE notation,

$$\underline{\varepsilon} = \mathbf{B} \mathbf{U}, \quad (21)$$

where, using Equation 18 to 20, the strain-displacement matrix  $\mathbf{B}$  is given by

$$\mathbf{B} = \frac{1}{h} \begin{bmatrix} 0 & 0 & 0 & 0 \\ 0 & -1 & 0 & 1 \\ -1 & 0 & 1 & 0 \end{bmatrix}. \quad (22)$$

The stiffness matrix can be written as

$$\mathbf{K}' = bt \int_{-h/2}^{h/2} \mathbf{B}^T \mathbf{E} \mathbf{B} \, dy, \quad (23)$$

where  $\mathbf{E}$  is the constitutive matrix for plane strain,

$$\mathbf{E} = \begin{bmatrix} \lambda + 2\mu & \lambda & 0 \\ \lambda & \lambda + 2\mu & 0 \\ 0 & 0 & \mu \end{bmatrix}. \quad (24)$$

The result of the integration in Equation 23 is:

$$\mathbf{K}' = \frac{bt}{h} \begin{bmatrix} \mu & 0 & -\mu & 0 \\ 0 & \lambda + 2\mu & 0 & -(\lambda + 2\mu) \\ -\mu & 0 & \mu & 0 \\ 0 & -(\lambda + 2\mu) & 0 & \lambda + 2\mu \end{bmatrix}. \quad (25)$$

This result is in agreement with the requirement that the P-wave and the S-wave travel independently of each other and with velocities given by Equation 3 and 4, respectively. The P-wave causes only vertical displacements, and the S-wave causes only lateral displacements, as illustrated in Figure 3. The stresses due to nodal displacements  $\mathbf{U}$  are given by

$$\underline{\boldsymbol{\sigma}}' = \mathbf{E} \mathbf{B} \mathbf{U} = \frac{1}{h} \begin{bmatrix} \lambda (V_4 - V_1) \\ (\lambda + 2\mu)(V_4 - V_1) \\ \mu (U_4 - U_1) \end{bmatrix}. \quad (26)$$

A device commonly used to represent viscous material damping is Rayleigh damping, in which the damping matrix is calculated as a linear combination of the mass and the stiffness matrix:

$$\mathbf{C}' = \alpha_R \mathbf{M}' + \beta_R \mathbf{K}', \quad (27)$$

where  $\alpha_R$  and  $\beta_R$  are constants.

### 5.3 The complete element

The complete free-field element is illustrated in Figure 4. Nodes 1 and 4 define the soil column element derived in the previous section. Nodes 2 and 3 both lie on the boundary of main model. These two nodes are coupled to the free field soil column through dashpots and springs (only normal dashpots are shown in Figure 4). Nodes 1 and 4 are not coupled to nodes 2 and 3, as information only travels from the soil column to the main model, not the other way.

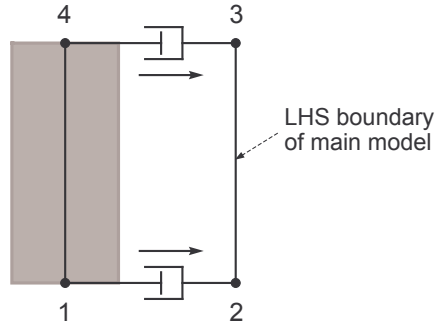


**Figure 4. The free field element when attached to the left-hand-side boundary of the main model.**

The full mass matrix  $\mathbf{M}$  for the free-field element is given in Appendix A; it is simply the soil column matrix  $\mathbf{M}'$  expanded to all eight degrees of freedom (nodes 2 and 3 do not have any mass associated with them).

The element applies the free-field boundary traction given by Equation 16 to the surface defined by nodes 2 and 3. Each of these nodes is associated with an area  $A = \frac{1}{2}ht$ . Using Equation 26, the discrete form of Equation 16 can be written as

$$\begin{aligned}
 P_x^{(2)} &= \frac{t}{2} [h\rho c_p (\dot{U}_1 - \dot{U}_2) + \ell_x \lambda (V_4 - V_1)] \\
 P_y^{(2)} &= \frac{t}{2} [h\rho c_s (\dot{V}_1 - \dot{V}_2) + \ell_x \mu (U_4 - U_1)] \\
 P_x^{(3)} &= \frac{t}{2} [h\rho c_p (\dot{U}_4 - \dot{U}_3) + \ell_x \lambda (V_4 - V_1)] \\
 P_y^{(3)} &= \frac{t}{2} [h\rho c_s (\dot{V}_4 - \dot{V}_3) + \ell_x \mu (U_4 - U_1)]
 \end{aligned} \tag{28}$$

where  $P_k^{(n)}$  is force applied to node  $n$  in direction  $k$ . This is a ‘lumped’ formulation; see Cohen and Jennings (1983) for a consistent force vector. Equation 28 is conveniently written in matrix form as

$$P = C''\dot{U} + K''U . \quad (29)$$

Expanding the structural matrices of the soil column (Equation 25 and 27) to all eight degrees of freedom, the internal forces in the soil column may be written as

$$R = C'\dot{U} + K'U . \quad (30)$$

Hence, using Equation 12, the static residual is given by

$$\begin{aligned} G &= (C'' - C')\dot{U} + (K'' - K')U \\ &= -C\dot{U} - KU \end{aligned} , \quad (31)$$

where the full damping matrix  $C$  and the full stiffness matrix  $K$  are given in Appendix A. It should be noted that both  $C$  and  $K$  are unsymmetrical. This is because the free-field soil column is not coupled to the main model. The residual  $F$  and the Jacobian  $J$  are now easily computed from Equation 11 and 14 respectively.

#### 5.4 Validation of the element

The main purpose of the following test was to show that the free-field element does not distort vertically propagating P- and S-waves. Two ABAQUS models were defined. Both models comprised of a flat site with three horizontal soil layers as shown in Figure 5 (a). The properties of the soil layers are given in Table 1. An acceleration time history was applied at the base of the models, and the solution was calculated using a fixed time step  $\Delta t = 0.01s$ .

Layer	A	B	C
Density (kg/m <sup>3</sup> )	2000	2400	2700
Young's modulus (MPa)	300	700	2000
Poisson's ratio	0.30	0.40	0.25

**Table 1. Properties used in the validation test.**

In the first model (Figure 5 (b)) the lateral boundaries were tied to each other such that the displacements of the LHS boundary were equal to those of the RHS boundary. This method is described in Zienkiewicz *et al.* (1989). It provides exact boundary conditions for a flat site. The second model (Figure 5 (c)) is identical to the first, except boundary conditions are modelled by the free-field element. Note that ABAQUS displays all user elements by the symbol  $\times$  at the first node.

Acceleration time histories recorded at the top of the models were compared and found to be almost equal (see Figure 6). The small differences may be due to the fact that ABAQUS employs

a different solution scheme for unsymmetrical systems. However, for engineering purposes, the loss of accuracy is negligible as demonstrated by the test.

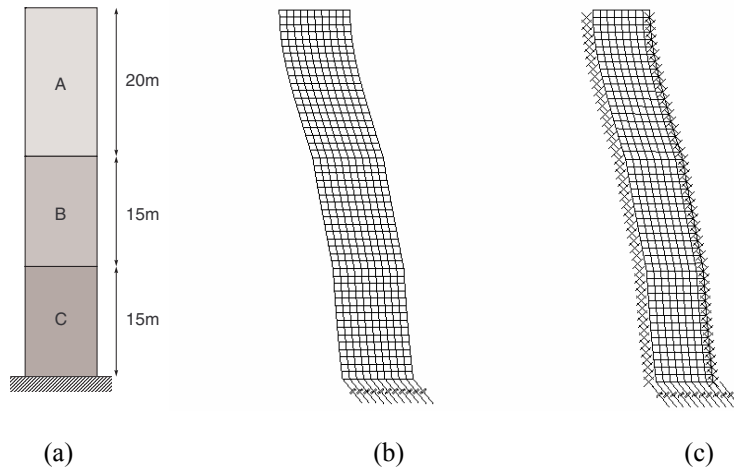


**Figure 5. (a) Stratigraphy; (b) ABAQUS model with tied boundaries; (c) ABAQUS model with free-field boundaries.**

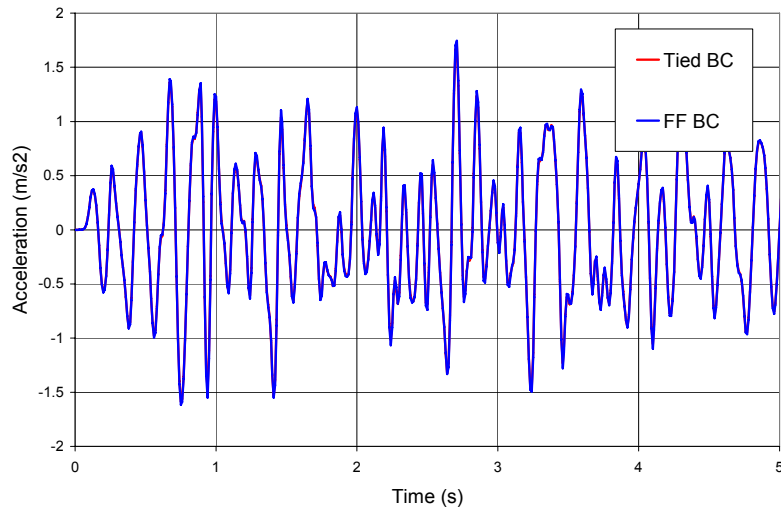


**Figure 6. Acceleration time history recorded at the top of the test models.**

## 6. Summary

This paper reviewed a number of absorbing boundary conditions for seismic analysis of civil engineering structures in time domain. Lysmer and Kuhlemeyer's viscous boundary was chosen for implementation due to the relative simplicity of the scheme, and its proven track record. However, the viscous boundary is not well suited for problems that involve evanescent waves. Future work should aim towards the implementation of a boundary condition that can absorb both oscillating and evanescent waves. The free-field boundary condition was defined as combination of the viscous boundary and the free-field soil column as proposed by Zienkiewicz *et al.* The scheme was implemented as new user element for implicit analysis in ABAQUS/Standard.

## 7. References

- Cohen, M. and P.C. Jennings, "Silent boundary methods for transient analysis", in: *Computational Methods for Transient Analysis*, eds. T. Belytschko and T.J.R. Hughes, Elsevier Science, 1983
- Cook, R.D., D.S. Malkus, M.E. Plesha, and R.J. Witt, *Concepts and Applications of Finite Element Analysis*, 4<sup>th</sup> ed., John Wiley & Sons, 2002
- Engquist, B. and A. Majda, "Radiation boundary conditions for acoustic and elastic wave calculations", *Communications on Pure and Applied Mathematics*, vol. 32, pp. 313 -357, 1979
- Guddati, M.N., "Continued-fraction absorbing boundary conditions for the wave equation", *Journal of Computational Acoustics*, vol. 8, no. 1, pp. 139 – 156, 2000
- Guddati, M.N., "Arbitrarily wide-angle wave equations for complex media", *Computer Methods in Applied Mechanics and Engineering*, vol. 195, pp. 65 – 93, 2006
- Higdon, R.L., "Radiation boundary conditions for elastic wave propagation", *SIAM Journal on Numerical Analysis*, vol. 27, no. 4, pp. 831 – 870, 1990
- Lindman, E.L., "Free space boundaries for the scalar wave equation", *Journal of Computational Physics*, vol. 18, pp. 66 – 78, 1975
- Love, A.E.H., *A Treatise on the Mathematical Theory of Elasticity*, 4<sup>th</sup> ed., Dover Publications, 1944
- Lysmer, J. and R.L. Kuhlemeyer, "Finite dynamic model for infinite media", *Journal of the Engineering Mechanics Division, Proc. ASCE*, vol. 95, no. EM4, pp. 859 – 876, 1969.
- Mulder, W.A., "Experiments with Higdon's absorbing boundary conditions for a number of wave equations", *Computational Geosciences*, vol. 1, p. 85 – 108, 1997
- Randall, C.J., "Absorbing boundary conditions for the elastic wave equation", *Geophysics*, vol. 53, no. 5, pp. 611 – 624, 1988



## 8.2 Damping matrix

$$\mathbf{C} = \begin{bmatrix} c_{11} & & & & & & & c_{17} \\ & c_{22} & & & & & & c_{28} \\ c_{31} & & c_{33} & & & & & \\ & c_{42} & & c_{44} & & & & \\ & & & & c_{55} & & c_{57} & \\ & & & & & c_{66} & & c_{68} \\ c_{71} & & & & & & c_{77} & \\ & c_{82} & & & & & & c_{88} \end{bmatrix}$$

where

$$\begin{aligned} c_{11} = c_{77} &= \alpha_R \frac{m}{2} + \beta_R \frac{bt\mu}{h}, & c_{17} = c_{71} &= -\beta_R \frac{bt\mu}{h} \\ c_{22} = c_{88} &= \alpha_R \frac{m}{2} + \beta_R \frac{bt(\lambda + 2\mu)}{h}, & c_{28} = c_{82} &= -\beta_R \frac{bt(\lambda + 2\mu)}{h} \\ c_{33} = c_{55} &= \frac{ht\rho c_p}{2}, & c_{31} = c_{57} &= -\frac{ht\rho c_p}{2} \\ c_{44} = c_{66} &= \frac{ht\rho c_s}{2}, & c_{42} = c_{68} &= -\frac{ht\rho c_s}{2} \end{aligned}$$

## 8.3 Stiffness matrix

$$\mathbf{K} = \begin{bmatrix} k_{11} & & & & & & & k_{18} \\ & k_{22} & & & & & & k_{28} \\ & & k_{32} & & & & & k_{38} \\ k_{41} & & & & & & k_{47} & \\ & k_{52} & & & & & & k_{58} \\ k_{61} & & & & & & k_{67} & \\ k_{71} & & & & & & k_{77} & \\ & k_{82} & & & & & & k_{88} \end{bmatrix}$$

where

$$\begin{aligned}
k_{11} = k_{77} &= \frac{bt\mu}{h} \quad , \quad k_{17} = k_{71} = -\frac{bt\mu}{h} \\
k_{22} = k_{88} &= \frac{bt(\lambda + 2\mu)}{h} \quad , \quad k_{28} = k_{82} = -\frac{bt(\lambda + 2\mu)}{h} \\
k_{32} = k_{52} &= \ell_x \frac{t\lambda}{2} \quad , \quad k_{38} = k_{58} = -\ell_x \frac{t\lambda}{2} \\
k_{41} = k_{61} &= \ell_x \frac{t\mu}{2} \quad , \quad k_{47} = k_{67} = -\ell_x \frac{t\mu}{2}
\end{aligned}$$